

Various Models for Pion Probability Distributions from Heavy-Ion Collisions

A.Z. Mekjian^{1,2*}, B.R. Schlei^{2,3†} and D. Strottman^{2‡}

¹*Rutgers University, Department of Physics, Piscataway, NJ 08854, USA*

²*Theoretical Division, DDT-DO, Los Alamos National Laboratory, Los Alamos, NM 87545, USA*

³*Physics Division, P-25, Los Alamos National Laboratory, Los Alamos, NM 87545, USA*

(July 29, 1998)

Various models for pion multiplicity distributions produced in relativistic heavy ion collisions are discussed. The models include a relativistic hydrodynamic model, a thermodynamic description, an emitting source pion laser model, and a description which generates a negative binomial distribution. The approach developed can be used to discuss other cases which will be mentioned. The pion probability distributions for these various cases are compared. Comparison of the pion laser model and Bose-Einstein condensation in a laser trap and with the thermal model are made. The thermal model and hydrodynamic model are also used to illustrate why the number of pions never diverges and why the Bose-Einstein correction effects are relatively small. The pion emission strength η of a Poisson emitter and a critical density η_c are connected in a thermal model by $\eta/\eta_c = e^{-m/T} < 1$, and this fact reduces any Bose-Einstein correction effects in the number and number fluctuation of pions. Fluctuations can be much larger than Poisson in the pion laser model and for a negative binomial distribution. The clan representation of the negative binomial distribution due to Van Hove and Giovannini is discussed using the present description. Applications to CERN/NA44 and CERN/NA49 data are discussed in terms of the relativistic hydrodynamic model.

PACS numbers: 24.10.Jv, 21.65.+f, 24.85.+p, 25.75.-q

I. INTRODUCTION

Pion multiplicity distributions produced in heavy ion collisions are of current interest for several reasons. First, pions are by far the main component of the produced particles in very high energy heavy ion collisions. For example, in the SPS experiments at CERN hundreds of pions are produced, and this number may go up considerably at RHIC energies. In the Landau hydrodynamic model, the number of pions scales at $S^{1/4}$ where $S = E_{\text{cm}}^2$. Secondly, pions are a useful tool for studying HBT effects coming from Bose-Einstein correlations. HBT two-particle correlation experiments give information about source parameters of the emitting system. Thirdly, if many pions are produced by a strongly emitting source at high enough density, a pion laser may be formed according to one model owing to Bose-Einstein symmetrization effects. Pions with a nonzero chemical potential can also show the phenomena of Bose-Einstein condensation at some critical density. Since Bose-Einstein condensation of a finite number of atoms in a harmonic oscillator or

laser trap has recently been seen, the possibility of seeing effects associated with the formation of a pion laser or an enhanced condensation into a ground state would be interesting. A comparison of Bose-Einstein condensation of atoms in a harmonic oscillator trap and the pion laser model will be given in this paper. Fourthly, the possibility of intermittency behavior in pion distributions has been a concern for over a decade. A distribution that is widely used to discuss intermittency is the negative binomial distribution, and a model which generates a negative binomial distribution will be developed in the framework of the present description. The clan representation for the negative binomial distribution due to Van Hove and Giovannini will also be discussed. This representation is a useful way of characterizing experimental data.

In this paper we present a unified description of several currently discussed models for evaluating pion distributions. Our main focus will be on four particular cases, but other possibilities exist and will be discussed briefly. The examples we will consider in detail are 1) a thermodynamic description, 2) a relativistic hydrodynamic model, 3) an emitting source model, and 4) a model which gives a negative binomial distribution. These cases cover a wide spectrum of possibilities. Thermodynamic descriptions have been extensively used [1]– [5] for the production of pions in heavy ion collisions and also are discussed in the quark matter meetings [4,5]. Emitting source models

*E. Mail: mekjian@ruthep.rutgers.edu

†E. Mail: schlei@LANL.gov

‡E. Mail: dds@LANL.gov

are reviewed in Refs. [6,7]. The emitting source model that we discuss in detail is originally due to Pratt [8] and discussed further in Refs. [9,10]. Application of the negative binomial distribution to high energy collision data can be found in Refs. [11]– [14], and its connection with intermittency are discussed in Refs. [15,16]. Hydrodynamic descriptions are also frequently applied to heavy ion collisions, and their descriptions appear in the quark matter proceedings, Refs. [4,5]. The relativistic hydrodynamic model gives a good description of single and double inclusive data from Cern experiments carried out by the CERN/NA44 and CERN/NA49 collaborations.

We will use an approach that initially was developed for cluster distributions [17]– [23], but applications to cycle class problems were noted [17] and further studied in more detail in Refs. [21]– [23]. Cycle class problems appear in Bose-Einstein and Fermi-Dirac statistics because the density matrix must be symmetrized or antisymmetrized in Feynman's path integral approach to statistical mechanics [24]. A detailed application of the approach discussed below to Bose-Einstein condensation phenomena can be found in Refs. [22,23]. The connection between cluster models and cycle class problems is shown in Fig. 1. Specifically, a cycle of length k corresponds to a cluster of size k , and the number of cycles of length k corresponds to the number of clusters of size k .

Application of results from cluster models to the theory of disordered systems can be found in Refs. [25,26]. Some of the results of this reference were connected to probability distributions which appear in *Quantum Optics*. Methods from *Quantum Optics* have been used by Weiner [27]– [29] *et al.* to discuss particle production and correlations in heavy ion collisions.

II. PION PROBABILITY DISTRIBUTIONS

In this section we will discuss several models of pion production in heavy ion collisions. These models, which are a thermodynamic description, a relativistic hydrodynamic model, an emitting source model, and a negative binomial model, can be described using a unified formalism. Before giving specific results, we will give some general expressions that we will use. These expressions were initially developed for the description of the fragmentation of nuclei into clusters. However, because of the correspondence between cycles and clusters shown in Fig. 1, the cluster results can be used to describe cycle class problems, and the pion production models that we consider can be re-expressed in such terms. This correspondence has already been illustrated in the description of Bose-Einstein condensation.

This section is divided into various subsections. First, we give some general results. Then we will apply these results to the cases mentioned above. Comparisons will

be made for the various cases and with other situations already discussed such as Bose-Einstein condensation.

A. General Results

In describing a fragmentation process, partitioning problems, or cycle class problems, a weight is given to each division of $A = \sum_k kn_k$. Figure 2 illustrates the possible divisions of $A = 4$. A vector $\vec{n} = (n_1, n_2, \dots, n_k, n_A)$ specifies the division where n_k is the number of clusters with k nucleons, cycles of length k , etc. A general block picture for \vec{n} is shown in Fig. 1, and the specific block pictures of $A = 4$ are shown in Fig. 2 along with cluster and cycle class divisions and harmonic oscillator excitations. The type of weight $W_A(\vec{n}, \vec{x})$ given to any \vec{n} that we will consider can be written as

$$W_A(\vec{n}, \vec{x}) = \frac{1}{Z_A(\vec{x})} \prod_k \frac{x_k^{n_k}}{n_k!} \quad (1)$$

Here $n_k!$ are Gibbs factorials, $Z_A(\vec{x})$ is the canonical partition function, and x_k is a function of thermodynamic quantities such as volume V , temperature T . This x_k was called a tuning parameter in Ref. [17], and a specific form $x_k = x/k$ was studied in detail in Refs. [17,18]. Other forms for x_k were used to study percolative features of simple statistical model [21] and Bose-Einstein condensation of atoms in a box [22] and atoms in a laser trap [23]. The form of x_k for the pion models to be discussed will be given below.

Given $W_A(\vec{n}, \vec{x})$ of the type of Eq. (1), various quantities are easily calculated. For example the ensemble averages of n_k , given by $\langle n_k \rangle = \sum W_A(\vec{n}, \vec{x}) n_k$, where the sum is over all partition of A , is simply [17,20]

$$\langle n_k \rangle = x_k \frac{Z_{A-k}(\vec{x})}{Z_A(\vec{x})} \quad (2)$$

This result can be easily understood heuristically by noting that the n_k times the Gibbs factorial $1/n_k!$ gives $1/(n_k - 1)!$. This operation removes one column of k blocks from Fig. 1. The sum over all partitions of A , which we call $\pi_A(\vec{n})$ in $\sum W_A(\vec{n}, \vec{x}) n_k$, then gives rise to the factor $Z_{A-k}(\vec{x})$. The x_k factor in Eq. (2) is from the shift $x_k^{n_k} = x_k x_k^{n_k-1}$ where the $x_k^{n_k-1}$ is the appropriate power of x_k for the partitions with one column of k blocks removed. The $Z_A(\vec{x})$ in Eq. (2) is present in $W_A(\vec{n}, \vec{x})$ and is in the final answer. Since the constraint $A = \sum_k kn_k$ always applies to any partition of A , then it is also true when written as $A = \sum_k k \langle n_k \rangle$. Substituting the result of Eq. (2) into this constraint equations gives $A = \sum_k k x_k Z_{A-k} / Z_A$, and rearranging terms results in the recursive relation

$$Z_A(\vec{x}) = \frac{1}{A} \sum_k k x_k Z_{A-k}(\vec{x}) \quad (3)$$

with $Z_0 = 1$. This recursive equation is a very simple way of obtaining $Z_A(\vec{x})$, and it applies to any $W_A(\vec{n}, \vec{x})$ of the form of Eq. (1). To use it, the x_k 's have to be specified. As an example $x_k = x/k$ gives [17,18]

$$Z_A(x) = x(x+1)\dots(x+A-1)/A! = \frac{\Gamma(A+x)}{\Gamma(x)A!} \quad (4)$$

The $Z_A(\vec{x})$ is the canonical partition function of a system of A objects (A nucleons, A atoms, ...). The grand canonical partition function $z(\vec{x}, u)$ is obtained from the canonical partition function $Z_A(\vec{x})$ or the weight $W_A(\vec{n}, \vec{x})$. For example, the generating function of $W_A(\vec{x}) = \sum_{\pi_A(\vec{n})} W_A(\vec{n}, \vec{x})$ is [17]

$$z(\vec{x}, u) \equiv \exp [ux_1 + u^2x_2 + u^3x_3 + \dots] = \sum_{A=0}^{\infty} W_A(\vec{x})u^A \quad (5)$$

The u is taken to be $u = e^{\beta\mu}$ in thermodynamics, where μ is the chemical potential. For $\mu = 0$, $u = 1$ and

$$z(\vec{x}) = \exp \left[\sum_{k=1}^{\infty} x_k \right] \quad (6)$$

The ratio

$$Z_A(\vec{x})/z(\vec{x}) = P_A(\vec{x}) \quad (7)$$

is the ratio of the canonical partition function to the grand canonical partition function. The mean and variance of A follow once the x_k 's are specified:

$$\langle A \rangle = \sum_k kx_k \quad (8)$$

and

$$\langle A^2 \rangle - \langle A \rangle^2 = \sum_k k^2 x_k. \quad (9)$$

These last two equations follow from Eq. (5) by differentiating this equation with respect to u and setting $u = 1$. These expressions form the main general results to be used in this paper. Other results can be found in Refs. [17]– [22].

B. Pion Distributions in a Thermal Model

We begin this subsection by first giving some well-known results on the thermal properties of an ideal gas of relativistic pions. Some of these results will then be used to motivate some ideas, developments, and comparisons to be made later. Moreover, since the thermal description is extensively used, many readers will recognize these results and this is helpful for the subsequent development of the choice of x_k for this particular model and other models to follow.

In a thermal model or in a description based on statistical mechanics, the distributions associated with pions are obtained from the assumption that an equilibrium is established in some interaction volume V at some temperature T . Specifically, statistical thermodynamics gives the Bose-Einstein occupancy factor

$$f(\epsilon) = \frac{1}{e^{\beta\epsilon} - 1} \quad (10)$$

for an energy level at ϵ and $\beta = 1/k_B T$. This result is based on the grand canonical ensemble with the pion chemical potential $\mu = 0$. For pions in a box of volume V , the thermal properties of pions can be obtained from the density of states factor Vd^3p/h^3 and from the energy ϵ , momentum \vec{p} , relation $\epsilon = (p^2 + m^2)^{1/2}$. In particular, with $\hbar = c = k_B = 1$, the following relations can be obtained for thermal pions:

$$\begin{aligned} \frac{N}{V} &= \frac{1}{2\pi^2} m^2 T \sum_{k=1}^{\infty} \frac{1}{k} K_2 \left(k \frac{m}{T} \right) \\ \frac{E}{V} &= \frac{1}{2\pi^2} m^3 T \sum_{k=1}^{\infty} \frac{1}{k} \left[\frac{3}{4} K_3 \left(k \frac{m}{T} \right) + \frac{1}{4} K_1 \left(k \frac{m}{T} \right) \right] \\ PV &= \frac{1}{2\pi^2} m^2 T \sum_{k=1}^{\infty} \frac{1}{k^2} K_2 \left(k \frac{m}{T} \right) \\ \frac{S}{V} &= ((E/V) + p) / T \end{aligned} \quad (11)$$

Here N/V is the total number density, E/V —the energy density, pV —the equation of state, and S/V —the entropy density of pions. The various K 's are MacDonald functions. The ultrarelativistic photon-like limit $m \rightarrow 0$ or $T \gg m$ and the nonrelativistic limit $\epsilon = p^2/2m + m$ can be obtained from these equations using the following limits for the MacDonald functions K_ν that appear. With $z = km/T$: $K_\nu(z) = (\Gamma(\nu)/2) / (1/2z)^\nu$ for $z \rightarrow 0$ and $K_\nu(z) = \sqrt{(\pi/2z)} e^{-z}$ for $z \rightarrow \infty$. Here $\Gamma(\nu)$ is a gamma function. In the above Eq. (11), the sum over k gives the corrections arising from Bose-Einstein or BE statistics, with the $k = 1$ term the Maxwell Boltzmann or MB limit. Specifically, the $k = 2, 3, \dots \infty$ give the enhancements coming from BE statistics. For example, for N/V the ratio $N/V / (N/V)_{\text{MB}} = \zeta(3)$ in the massless pion limit. Here $(N/V)_{\text{MB}}$ is the $k = 1$ term only. The $\zeta(3) = 1.2$ is the Riemann zeta function. The results of Eq. (11) arise when the occupancy factor of Eq. (10) is expanded as a power series $f(\epsilon) = e^{-\beta\epsilon} (1 + e^{-\beta\epsilon} + e^{-2\beta\epsilon} + \dots)$. The integrals over $(Vd^3p/h^3)e^{-k\beta\epsilon}$ with $\epsilon = \sqrt{p^2 + m^2}$ give rise to the various K 's.

The probability of having n_k pions in level k , given that the mean number in that level is $\langle n_k \rangle = 1 / (e^{\beta\epsilon_k} - 1)$ is the geometric distribution [30]

$$p(n_k) = \frac{\langle n_k \rangle^{n_k}}{(\langle n_k \rangle + 1)^{n_k + 1}} \quad (12)$$

The $\langle n_k \rangle = \sum_{n_k=0}^{\infty} p(n_k) n_k$ and $\langle n_k^2 \rangle - \langle n_k \rangle^2$ is

$$\langle n_k^2 \rangle - \langle n_k \rangle^2 = \langle n_k \rangle (1 + \langle n_k \rangle) \quad (13)$$

The Poisson limits is $\langle n_k^2 \rangle - \langle n_k \rangle^2 = \langle n_k \rangle$ and is realized when MB statistics applies. The above expression on fluctuations pertain to a particular energy level. We now turn to an evaluation of the fluctuations in the total number of pions and its associated probability distribution. Such quantities are important in an event-by-event analysis of data. The probability of N -pions is given by the ratio of the canonical partition function, Z_N , to the grand canonical partition function z , with $z = \sum_{N=0}^{\infty} Z_N$ and $Z_O = 1$. To obtain Z_N, z we use results from Sec. II.A with $u = e^{\beta\mu} = 1$. For a thermal model the choice of x_k is

$$x_k = \frac{VT^3}{2\pi^2} \left(\frac{m}{T}\right)^2 \frac{1}{k^2} K_2\left(k\frac{m}{T}\right) \quad (14)$$

Later, we will give other choice of x_k . That this is the correct choice follows from $\langle N \rangle = \sum_k k x_k$ where $\langle N \rangle / V$ in the grand canonical ensemble is given by Eq. (11). Also $z = e^{PV/T} = e^{\sum_k x_k}$ where $PV/T = \sum_k x_k$ follows also from Eq. (11), and $z = e^{\sum_k x_k}$ was a result developed in Sec. II.A. The result for $z = e^{\sum_k x_k}$ can be expanded to give the $W_N(\vec{x})$ of Eq. (5) and its associated $W_N(\vec{n}, \vec{x}) = \prod [x_k^{n_k} / n_k! / Z_N(\vec{x})]$ of Eq. (1). The $W_N(\vec{n}, \vec{x})$ is the weight given to $\vec{n} = (n_1, n_2 \dots n_A)$ in a cycle class decomposition of a permutation. For example the permutation

$$\begin{pmatrix} 1 & 2 & 3 & 4 & 5 & 6 & 7 \\ 1 & 3 & 2 & 4 & 7 & 5 & 6 \end{pmatrix} \quad (15)$$

has two cycles of length 1 which are $1 \rightarrow 1$ and $4 \rightarrow 4$, one cycle of length 2 which is $2 \rightarrow 3 \rightarrow 2$, and one cycle of length 3 which is $5 \rightarrow 7 \rightarrow 6 \rightarrow 5$. The cycles appear in Feynman's path integral density matrix approach in *Statistical Mechanics* [24], and permutations appear because the density matrix must be symmetrized. An example of this approach to the ideal Bose gas in a box [22] and to the ideal Bose gas in a harmonic oscillator trap [23] shows the utility of the recurrence relation of Eq. (3) in obtaining the canonical partition function $Z_N(\vec{x})$ and all its associated thermodynamic quantities. We will briefly summarize these two cases in the next section.

Using this choice of x_k , the probability of N pions is $P_N = Z_N/z$ where Z_N is obtained from Eq. (3) with x_k given by Eq. (14). The fluctuations $\langle N^2 \rangle - \langle N \rangle^2 = \sum k^2 x_k$. An alternative method for obtaining P_N was recently given by Becattini, Giovannini, and Lupia [31]. They used projection methods to obtain P_N which involves taking N -derivatives of z with respect to u and

setting $u = 0$. Specifically

$$P_N = \frac{1}{N!} \lim_{w \rightarrow 0} \frac{d^N}{dw^N} \exp \left[-\frac{V}{2\pi^2} \int d^3p \log \left(1 - e^{-\epsilon/T} \omega \right) \right] \quad (16)$$

Table 1 summarizes P_N for $T = 163$ MeV, $V = 22.5$, and $m/T = 0.85$. This choice generates the same P_N distribution given in Ref. [32]. Here the P_N 's are calculated by the simple recurrence relation of Eq. (3). Computationally, Eq. (3) is very easy to work with since computers evaluate recursive relations quickly as well as the sums for $\langle N \rangle$ and $\langle N^2 \rangle - \langle N \rangle^2$ that appear in Eq. (8).

Two limiting behavior of x_k are of interest. In the ultra-relativistic limit or massless pion limit, the x_k of Eq. (14) is simply

$$x_k = \frac{V}{\pi^2} T^3 \frac{1}{k^4} \quad (17)$$

and in the nonrelativistic limit

$$x_k = \frac{V}{\lambda_T^3} e^{-km/T} \frac{1}{k^{5/2}} \quad (18)$$

where $\lambda_T = h/(2\pi mT)^{1/2}$. The factor $e^{-km/T}$ is the Boltzmann factor cost function for creating k -pions, and this factor arises from the mass of the pion. We will introduce a quantity τ , where $x_k \sim 1/k^\tau$. In cluster models τ is Fisher's critical exponent [32]. In Eq. (17) $\tau = 4$ and in Eq. (18) $\tau = 5/2$.

C. Relativistic Hydrodynamic Model and Applications to CERN/NA44 and CERN/NA49 Experiments

We also calculated the pion probability distribution using a relativistic hydrodynamic model: HYLANDER-C [28]. This particular model belongs to the class of models which apply 3+1-dimensional relativistic one-fluid-dynamics. It provides fully three-dimensional solutions of the hydrodynamical relativistic Euler-equations [35]. HYLANDER-C and its earlier version, HYLANDER [33], have been successfully applied to various heavy-ion reactions at SPS energies. HYLANDER-C and HYLANDER were used to reproduce [36] simultaneously mesonic and baryonic rapidity and transverse momentum spectra of the $S + S$ reaction at 200 AGeV. Corresponding measurements have been performed by the NA35 Collaboration [37]. Based on the successful description of the measured single-inclusive spectra, predictions for Bose-Einstein correlation (BEC) functions [38,39] were made. Those predictions turned out to agree quantitatively with the measurements [40,41]. The model also reproduces the photon data for $S + Au$ collisions at SPS energies [42] and gives a simple explanation for the "soft- p_\perp puzzle" [43] and the complex behaviour of the radii extracted from pion and kaon correlations and explains the difference in

the extracted radii for pions and kaons in terms of a cloud of pions due to the decay of resonances which surrounds the fireball (pion halo) [38].

In the following, we discuss some further results [34] for 158A GeV Pb + Pb collisions measured by the CERN/NA44 [44,45] and CERN/NA49 Collaborations [46]. The by HYLANDER-C reproduced Pb+Pb data have been obtained while using an equation of state (EOS) with a phase transition to a quark-gluon plasma at a critical temperature $T_C = 200 \text{ MeV}$ (*cf.* Refs. [47], [29] and Refs. therein). This EOS does not depend on the baryon density, and thus the freeze-out energy density translates directly into a fixed freeze-out temperature T_f . The choice for the freeze-out temperature is in these calculations, $T_f = 139 \text{ MeV}$.

The number of thermal pions (π^+ , π^- , and π^0) that are produced in the model calculations is 853. In particular, this number does not include any resonance decay contributions. But this total number of thermal pions includes the Bose-Einstein enhancement. To be specific, the thermal pion spectra are calculated by evaluating the integral

$$E \frac{dN}{d^3p} = \frac{1}{(2\pi)^3} \int_{\Sigma} \frac{p^\mu d\sigma_\mu(x'_\mu)}{\exp\left[\frac{p^\mu u_\mu(x'_\mu)}{T_f(x'_\mu)}\right] - 1}, \quad (19)$$

where $d\sigma^\mu$ is the differential volume element and the integration is performed over the freeze-out hypersurface, Σ . $u^\mu(x)$ and T_f are the four velocity of the fluid element at point x and the freeze-out temperature, respectively. $p^\mu = (E, \vec{p})$ is the four-momentum of a pion.

By expanding the Bose-Einstein occupation factor in terms of a Maxwell-Boltzmann factor and a series of higher order corrections, we can obtain the distribution of x_k 's which are summarized in Table 2.

Using these results for x_k , the fluctuation in the thermal pions is $\langle N^2 \rangle - \langle N \rangle^2 = \sum k^2 x_k = 312.97$ or a 20% enhancement over the Poisson result of $x_1 = 260$. The probability distribution associated with the thermal pions is obtained from $P_N = Z_N/z$ where Z_N is given by Eq. (3) and z is given by Eq. (6). Figure 3 shows the result for P_N , which is a perfect Gaussian distribution (solid line) with mean $\langle N \rangle = 283.9$ and variance $\langle N^2 \rangle - \langle N \rangle^2 = 312.97$.

D. Some Special Examples

In this subsection, we will illustrate some of the general results of Sec. II.A with three specific examples. For massless particles in a box of sides L in d -dimensions (neglecting spin), the x_k is

$$x_k = \frac{L^d}{2^{d-3}\pi^{d-1}} \left(\frac{k_B T}{\hbar c}\right)^d \frac{1}{k^\tau} \equiv \frac{x_d}{k^\tau} \quad (20)$$

where $\tau = d + 1$. Then $z = \exp[x_d \zeta(\tau)]$, $\langle N \rangle = x_d \zeta(d)$ and $\langle N^2 \rangle - \langle N \rangle^2 = x_d \zeta(d-1)$ with $\zeta(n) = \sum_{k=1}^{\infty} 1/k^n$. Some values of $\zeta(n)$ that often appear in statistical mechanics are $\zeta(1) = \infty$, $\zeta(2) = \pi^2/6 = 1.645$, $\zeta(3) = 1.202$, $\zeta(4) = \pi^2/90 = 1.082$, $\zeta(3/2) = 2.612$. In two dimensions $\langle N^2 \rangle - \langle N \rangle^2 = \infty$ so that the fluctuations of massless particles becomes large.

For nonrelativistic atoms in a box [22] in d -dimensions

$$x_k = \frac{x}{k^\tau} + \frac{1}{k} \quad (21)$$

with $\tau = d/2 + 1$, $x = L^d/\lambda_T^d$, $\lambda_T = h/(2\pi mT)^{1/2}$. Condensation occurs in $d = 3$ at $x = x_c = A/\zeta(3/2) = V/\lambda_{T_c}^3$ in the limit $A, V \rightarrow \infty$. Manifestation of this Bose-Einstein condensation are 1) a power law distribution of cycle lengths [21,22]: $\langle n_k \rangle \sim 1/k^{5/2}$, 2) the specific heat C_V has a cusp [30], and 3) the ground state occupancy $n_{G.S.}$ becomes macroscopically large [30]: $n_{G.S.}/A = 1 - x/x_c = 1 - (T/T_c)^{3/2}$, for $T \leq T_c$. The T_c is determined by the density A/V from $A/\zeta(3/2) = V/\lambda_{T_c}^3$. For $d = 1, 2$ $T_c \rightarrow 0$ so that there is no sudden condensation at a nonzero T . The occupancy of any level with energy ϵ_k is

$$n_k = \sum_{k=1}^A e^{-\beta \epsilon_k} \frac{Z_{A-k}}{Z_A} \quad (22)$$

For $A \rightarrow \infty$, $Z_{A-k}/Z_A \rightarrow e^{\beta \mu k}$ and thus we obtain the well-known occupancy factor

$$n_k = \frac{1}{e^{\beta(\epsilon_k - \mu)} - 1}. \quad (23)$$

As $T \rightarrow T_c$, $\mu \rightarrow \epsilon_0 \equiv 0$.

For atoms in a laser trap given by a harmonic oscillator well with frequency ω and level spacing $\hbar\omega$ [23]

$$x_k = \frac{1}{k} \frac{x^{kd/2}}{(1-x^k)^d} \quad (24)$$

where $x = e^{-\hbar\omega/k_B T}$. For small x

$$x_k = \frac{x^{kd/2}}{k^{d+1}} \left(\frac{k_B T}{\hbar\omega}\right)^d$$

There is no condensation at nonzero T for $d = 1$, but there is condensation for $d = 2, 3$ at $T_c \neq 0$.

E. Emitting Source, Pion Laser Model

A simple and exactly solvable emitting source models for pions was first introduced by S. Pratt [8]. The model has an interesting feature. Namely, a Poisson emitter of pions can behave like a pion laser when Bose-Einstein symmetrization effects are included. A manifestation of this behavior is a large enhancement in the number of

pions. This enhancement is into a zero momentum state and is similar to Bose-Einstein condensation of atoms in a box which also condense into the zero momentum state. An important result of this condensation is a reduction in the intercept in the two particle correlation functions. Such effects were discussed in Refs. [27]– [30]. Recently Csörgö and Zimány [10] have given simple exact expressions for Pratt’s model. Some simple results were also presented by Chao, Gao, and Zhang [9]. This subsection presents some further discussions of this model using results from Sec. II.A when applied to this case and shows some similarities with the Bose-Einstein condensation of atoms in a laser trap as given by Eq. (24).

First, we will give expressions for x_k . Once x_k is given, then all the general results of Sec. II.B apply. In Pratt’s model, η is the mean pion multiplicity generated by a Poisson emitter. Then, in the Poisson limit, the probability of having N pions is $P_N = (\eta^N/N!) e^{-\eta}$. This is also the result of the thermal model of Sec. II.B in the Maxwell-Boltzmann limit, where $\eta = x_1 = (VT^3/2\pi^2)(m/T)K_2(m/T)$. Corrections to this result obtained from Bose-Einstein symmetrization effects can be developed by evaluating a quantity x_k (called C_k in Ref. [8]). The C_k are referred to as combinatorials [10]. The importance of combinatorials can be found in the work of Gyulassy and Kaufman [48,49]. While the x_k of the thermal model is given by Eq. (14), in the emitting source model x_k is given by evaluating

$$x_k = \frac{\eta^k}{k} \int \prod_{i=1}^k d^3\vec{x}_i d^3\vec{p} \prod_{i=1}^{k-1} d^3 p_i e^{i\Sigma(\vec{p}_{i-1} - \vec{p}_i) \cdot \vec{x}_i} \times \prod_{i=1}^k s\left(\frac{1}{2}(p_{i-1} + p_i), x_i\right) \quad (25)$$

where $p_0 = p = p_k$ and $x_1 = \eta$. We neglect any temporal dependence to keep the discussion simple.

The $s(\vec{p}, \vec{x})$ is the source strength. As in Ref. [8] this source strength is taken to be a thermal Gaussian of the form

$$S(\vec{p}, \vec{x}) = \frac{1}{((2\pi)^2 R^2 m T)^{3/2}} e^{-\vec{P}^2/2mT + \vec{x}^2/2R^2} \quad (26)$$

For this choice of $s(\vec{p}, \vec{x})$, the evaluation of the x_k ’s can be done analytically [9]. We now give a discussion of the limiting behavior of x_k before giving the general behavior. For small k and $R^2/2 \gg 1/8mT$ (typically $R^2/2 \sim 6$ and $1/8mT \sim 1/6$)

$$x_k = (R^2 m T)^{3/2} \left(\frac{\eta}{(R^2 m T)^{3/2}} \right)^k \frac{1}{k^4} \quad (27)$$

Thus $x_k \sim 1/k^4$ and $\tau = 4$ for small k . For large k

$$x_k = \frac{1}{k} \left(\frac{\eta}{\eta_c} \right)^k \quad (28)$$

Now $x_k \sim 1/k$ and $\tau = 1$. The η_c is given by

$$\eta_c = \left(R^2 m T + \sqrt{R^2 m T} + \frac{1}{4} \right)^{3/2} \quad (29)$$

Table 3 gives some values of x_k for $R^2/2 = 6$ and $1/8mT = 1/6$.

The general behavior for x_k was explicitly written by Csörgö and Zimány [10], and is

$$x_k = \frac{\eta^k}{k} \frac{1}{\left(\gamma_+^{k/2} - \gamma_-^{k/2} \right)^3} \quad (30)$$

with $\gamma_{\pm} = 1/2 (1 + y \pm \sqrt{1 + y})$ and $y = 2R^2 m T - 1/2$.

The $\eta_c = \gamma_+^{3/2}$ in this notation. We rewrite this as

$$x_k = \left(\frac{\eta}{\eta_c} \right)^k \frac{1}{k \left(1 - \left(\left(\frac{\gamma_-}{\gamma_+} \right)^{1/2} \right)^k \right)^3} \quad (31)$$

to illustrate its close relation to atoms in a laser trap as given by Eq. (24). For $d = 3$, Eq. (24) gives

$$x_k = \frac{x^{3k/2}}{k(1 - x^k)^3} \quad (32)$$

with $x = e^{-\hbar\omega/k_B T}$.

Once the x_k ’s are given, the $z = \exp[\sum x_k]$, $\langle N \rangle = \sum k x_k$, $\langle N^2 \rangle - \langle N \rangle^2 = \sum k^2 x_k$ and $P_N = z_N/z$ follow with Z_N given by the recurrence expression of Eq. (3). Since $x_k = 1/k(\eta/\eta_c)^k$ for large k , $\langle N \rangle \rightarrow \infty$ when $\eta \geq \eta_c$. At $\eta = \eta_c$ the $\langle N \rangle \sim \sum 1/k$ which diverges logarithmically. We now compare these results with thermal models. In thermal models, x_k is given by Eq. (14) and its nonrelativistic and ultrarelativistic limits in Eq. (17) and Eq. (18). No divergence in $\langle N \rangle$ occurs in either the ultrarelativistic limit where $\langle N \rangle = (V/\pi^2) T^3 \zeta(3)$, or the nonrelativistic limit where $\langle N \rangle = (V/\lambda_T^3) g_{3/2}(m/T)$ with $g_{3/2}(m/T) = \sum (e^{-m/T})^k / k^{3/2}$. Note, however, that fluctuations, $\langle N^2 \rangle - \langle N \rangle^2$, in the two-dimensional ultrarelativistic case discussed in Sec. II.C can be infinite. To further illustrate the difference, we note that in the thermal model all x_k ’s are given by Eq. (14) so that $x_1 \equiv \eta$ is not independent of V, T, m where $V \sim R^3$. Table 4 shows values of x_k for $V = \frac{4\pi}{3} R^3$ with $R^2/2 = 6$ and $mT = 3/4$. Using $\eta = x_1$, the x_k can be rewritten as $x_k \sim \eta^k$ and the results are also shown when written in this form. The results of Table 4 are very similar to Table 3. However, the large x_k limit is $(V/(\lambda_T^3 \cdot k^{5/2})) e^{-km/T}$. If we take x_1 to be this result with $k = 1$, the $x_k = (1/k^{5/2}) (\eta/\eta_c)^k$ with $\eta_c = V/\lambda_T^3 \sim (R^2 m T)^{3/2}$, which is similar to Eq. (29).

Note that $\eta = \eta_c e^{-m/T}$ so that $\eta/\eta_c = e^{-m/T} < 1$. Consequently, the sum $\sum x_k k = \langle N \rangle$ always converges. Thus

there can be no result $\langle N \rangle \rightarrow \infty$. The Boltzmann factor $e^{-m/T}$ suppresses the property $\langle N \rangle \rightarrow \infty$. This hidden connection between η , η_c , and $\eta/\eta_c < 1$ is not present in the pion laser model which treats η as independent of η_c or x_1 as independent of the other x_k 's. The thermal model has this connection and shows why no divergence in $\langle N \rangle$ ever occurs in the thermal model. Similar conclusions also apply to the relativistic hydrodynamic model.

F. Negative Binomial Distribution

As we have seen, pion probability distributions are determined once the choice of the x_k 's is specified. The thermal equilibrium model specifies a particular form for x_k as does the emitting source model. Bose atoms in a box or laser trap also can be discussed in terms of x_k . In this subsection we will present a choice for x_k which results in a negative binomial distribution. The choice given below is partly motivated by results from the other models. The negative binomial is a probability distribution that is frequently used to characterize pion yields [11]–[13]. It has also been used in the discussion of intermittency [15,16]. Van Hove and Giovannini [11]–[13] has given a clan model representation of it which will also be mentioned.

The various forms for x_k that we have encountered so far in this paper and also in the application of this approach to cluster yields suggest looking at a behavior for x_k given by

$$x_k = ay^k/k^\tau \quad (33)$$

For example, the nonrelativistic thermal model has $a = V/\lambda_T^3$, $y = e^{-m/T}$, and $\tau = 5/2$. The ultrarelativistic thermal model has $a = \frac{V}{\pi^2}T^3$, $y = 1$, and $\tau = 4$. The emitting source model, for small k , is $a = (R^2mT)^{3/2}$, $y = \eta/(R^2mT)^{3/2}$, $\tau = 4$ and is $a = 1$, $y = \eta/\eta_c$, $\tau = 1$ for large k . We will now show that the choice

$$x_k = ay^k/k, \quad (34)$$

which has $\tau = 1$, generates a negative binomial probability distribution. This way of generating a negative binomial distribution can be found in Ref. [50], more recently in Ref. [51], and was used in Refs. [17] and [20]. The a and y will be related to the mean number of pions and to their fluctuations. We will also connect them to the clan variables of Van Hove. Using results from Ref. [17] and Sec. II.A, the following behavior for various relevant quantities are obtained. First, the grand canonical partition function $z = \exp(\sum_k x_k) = 1/(1-y)^a$ which can easily be verified by noting $\sum_k ay^k/k = -a \log(1-y)$. The canonical partition function Z_n can be obtained and is [17] $Z_N = y^N \Gamma(a+N)/\Gamma(a)N!$ —see also Eq. (4). The extra y^N that appears here is from the y^k in x_k . Note that

$\prod_k (y^k)^{n_k} = y^N$ since $\sum_k kn_k = N$, where the $\prod_k (y^k)^{n_k}$ appears in $W_A(\vec{n}, \vec{x})$ of Eq. (1). One way to obtain this result for Z_N is directly from the recurrence relation of Eq. (3). The mean number of pions can be obtained from $\sum_k kx_k$ and is

$$\langle N \rangle = \frac{ay}{1-y} \quad (35)$$

The variance follows from $\langle N^2 \rangle - \langle N \rangle^2 = ay/(1-y)^2$ or

$$\langle N^2 \rangle - \langle N \rangle^2 = \langle N \rangle \left(1 + \frac{\langle N \rangle}{a} \right) \quad (36)$$

The result of Eq. (36) is the result for the variance of a negative binomial distribution. This result is also similar to that of Eq. (13) when $a = 1$, but Eq. (13) refers to fluctuations in a particular level k , while Eq. (36) has no reference to a level. The fluctuations can be much larger than Poissonian because of the factor $(1 + \langle N \rangle/a)$. To see that the probability distribution associated with this model ($x_k = ay^k/k$) is indeed a negative binomial distribution, the $P_N = Z_N/z$ can be easily evaluated and rewritten as

$$P_N = \binom{N+a-1}{N} \left(\frac{1}{1+\frac{\langle N \rangle}{a}} \right)^a \left(\frac{\langle N \rangle/a}{1+\frac{\langle N \rangle}{a}} \right)^N \quad (37)$$

The result of Eq. (37) is the standard form of the negative binomial distribution.

An interesting transformation of the negative binomial is to a set of clan variables N_c, n_c , given by [13]

$$\begin{aligned} N_c &= a \log \left(1 + \frac{\langle N \rangle}{a} \right) \\ n_c &= \frac{\langle N \rangle}{N_c} \end{aligned} \quad (38)$$

The N_c equals the average number of clans, and n_c is the average number of particles in a clan. The variables N_c, n_c are a useful way of analyzing experimental data. In terms of y and $z = 1/(1-y)^a$

$$\begin{aligned} N_c &= \log z \\ n_c &= -\frac{y}{(1-y)\log(1-y)} \end{aligned} \quad (39)$$

Thus n_c only depends on y and N_c is simply connected to z . Note that in thermodynamics (see also Sec. II.B), the grand canonical partition function z is connected to the equation of state. Specifically, $pV/k_B T = \log z$ so that $pV = N_c k_B T$ if this connection is made.

G. Other Models

Besides the choice $\tau = 1$, other choices for τ can be solved. Many of these other choices were studied in the

framework of cluster models [22], but the results obtained also apply to particle production of bosons. Some discussion of these issues can be found in Ref. [25] where results from a somewhat general theory of disordered systems were connected to distributions used in particle physics and quantum optics.

III. CONCLUSIONS

This paper discusses several models of pion production in a unified way by showing that they are different choices of a quantity which we called x_k . The models considered are a thermal description of pion production, a relativistic hydrodynamic model, an emitting source pion laser model, and a model that gives rise to a negative binomial distribution. The results of these models are compared with each other. Comparisons are also made with Bose-Einstein condensation of Bose particles or atoms trapped in a harmonic oscillator well and in a box of d -dimensions. The quantity x_k appears in the weight given to each cycle class decomposition of the symmetric group. The index k is the length of a cycle. The cycle classes appear when the density matrix is symmetrized as in Feynman's path integral approach to statistical mechanics. The quantities x_k , $k = 1, 2, 3, \dots$ completely determine the behavior of the system as discussed in Sec. II.A. Specifically the mean number of pions and their fluctuations are just moments of the x_k distribution. The grand canonical partition function z is also simply obtained from these x_k 's, and the canonical partition function Z_N can be obtained by a simple recursive procedure which contains the x_k . The probability of N -pions is $P_N = Z_N/z$. These methods and relations were initially used by one of us in cluster problems [17]–[22] and subsequently applied to Bose-Einstein cycle class problems [22,23]. They were also used in a discussion of the pion laser model in Refs. [8]–[10]. The two problems, cycle class and clusters, can be mapped into one another as shown in Fig. 1. Specifically the index k is either the cluster size or cycle length, and n_k is either the number of cycles of length k or the number of clusters with k nucleons. After presenting various general expressions, specific cases are discussed and compared. We started with the thermal model because of its long history and its widespread use in heavy ion collisions. The thermal model was used to motivate some of the quantities, such as the x_k 's that also appear in the other cases that are considered. The role of the Boltzmann factor $e^{-km/T}$ in x_k , which represents the cost function for making k -pions, is important in the thermal model. The mean number of pions, their fluctuations, and the probability distribution for N -pions are discussed and compared with Poisson results. The results for a relativistic hydrodynamic model are also discussed. The relativistic hydrodynamic model is used in the analysis of CERN/NA44 and CERN/NA49 data.

The probability distribution for thermal pions is shown to be a Gaussian distribution. The fluctuations in pions is about 20% above the Poisson limit. This result of slightly enhanced fluctuations is also consistent with thermal model results.

The emitting source model of S. Pratt is next discussed. It has an interesting feature of the possibility of large departures from Poissonian results. This model also has some other interesting properties that are not present in the thermal and hydrodynamic models. Namely, a critical pion density η_c exists and, if the Poisson emission strength η equals this density, an infinite number of pions results from Bose-Einstein enhancement factors. The thermal and hydrodynamic models lack this property because $\eta \sim \eta_c e^{-m/T}$. Some result of the emitting source model are shown to be similar to Bose-Einstein condensation in a laser trap when this trap is taken to be a three-dimensional harmonic oscillator well. Another distribution which can have large fluctuations above Poisson results is the negative binomial distribution. The clan representation of the negative binomial distribution, introduced by Van Hove and Giovannini, is discussed in terms of quantities that appear in the specification of the x_k 's. The clan representation is a useful way of characterizing data, and it is compared with the thermal model results.

This work has been supported by the U.S. Department of Energy.

-
- [1] E. Fermi, *Prog. Theor. Phys.* **5**, 570 (1950); *Phys. Rev.* **92**, 452 (1953).
 - [2] R. Hagedorn, *Cargese Lectures in Physics VI*, ed. E. Schatzman (Gordon and Breach, NY 1973).
 - [3] Hot Hadronic Matter NATO Series, Series B, Physics V.346, J. Letessier, H.H. Gutbrod, and J. Rafelski ed. (Plenum Press N.Y. 1995).
 - [4] Quark Matter '96, Proceedings of the Twelfth International Conference on Ultra-Relativistic Nucleus-Nucleus Collisions, Heidelberg, Germany, 20-24 May, 1996, *Nucl. Phys.* **A610**, 1c - 572c (1996).
 - [5] Quark Matter '97, Proceedings of the Thirteenth International Conference on Ultra-Relativistic Nucleus-Nucleus Collisions, Tsukuba, Japan, 1-5 December, 1997, unpublished.
 - [6] D. H. Boal and C. K. Gelbke, *Rev. of Modern Phys.* **V 62**, 553 (1990).
 - [7] R.M. Weiner, "Bose-Einstein Correlations in Particle and Nuclear Physics - A Collection of Reprints", John Wiley & Sons (1997).
 - [8] S. Pratt, *Phys. Lett. B* **301**, 159 (1993).
 - [9] W. Q. Chao, C. S. Gao, Q. H. Zhang, *J. Phys. G. Nucl. Part. Phys.* **21**, 847 (1995).
 - [10] T. Csörgö and J. Zimányi, CU-TP-818/1977 and *Phys. Rev. Lett.* **80**, 916 (1998).
 - [11] L. Van Hove and A. Giovannini, *Z. Phys. C* **30**, 391 (1986).

- [12] A. Giovannini, *Nuovo Cimento* **10A**, 713 (1972); **24A**, 421 (1974).
- [13] L. Van Hove, *Phys. Lett. B* **232**, 509 (1989).
- [14] P. Carruthers and C. C. Shih, *Phys. Lett.* **127B**, 242 (1983).
- [15] A. Bialas and R. Peschanski, *Nucl. Phys. B* **272**, 703 (1986); *B* **306**, 857 (1988).
- [16] A. Bialas, *Nucl. Phys. A* **545**, 282 (1992).
- [17] A. Z. Mekjian, *Phys. Rev. Lett.* **64**, 2125 (1990); *Phys. Rev.* **41**, 2103 (1990).
- [18] A. Z. Mekjian and S. J. Lee, *Phys. Rev. A* **44**, 6294 (1991).
- [19] K. C. Chase and A. Z. Mekjian, *Phys. Rev. Lett.* **75**, 4732 (1995).
- [20] S. J. Lee and A. Z. Mekjian, *Phys. Rev. C* **45**, 1284 (1992); *Phys. Rev. C* **50**, 3025 (1994); *Phys. Lett. A* **149**, 7 (1990).
- [21] K. C. Chase and A. Z. Mekjian, *Phys. Lett. B* **379**, 50 (1996).
- [22] K. C. Chase and A. Z. Mekjian, *Phys. Rev. C* **49**, 2164 (1994).
- [23] K. C. Chase, A. Z. Mekjian, and L. Zamick, "Canonical and Microcanonical Ensemble Approaches to Bose-Einstein Condensation: The Thermodynamics of Particles in Harmonic Traps," Rutgers Univ. preprint, cond-mat/9708070.
- [24] R. P. Feynman, *Statistical Mechanics: A Set of Lectures, Frontiers in Physics* (Benjamin/Cummings, Reading, MA, 1972).
- [25] A. Z. Mekjian and K. C. Chase, *Phys. Lett. A* **229**, 840 (1997).
- [26] K. C. Chase, P. Bhattacharya, and A. Z. Mekjian, *Phys. Rev. C* **57**, 882 (1998).
- [27] I. V. Andreev, M. Plümer, and R. M. Weiner, *Int. Journ. of Mod. Phys. A* **8**, 4577 (1993).
- [28] B.R. Schlei, *Heavy Ion Phys.* **5**, 403 (1997).
- [29] U. Ornik, M. Plümer, B.R. Schlei, D. Strottman, R.M. Weiner, *Phys. Rev. C* **54**, 1381 (1996).
- [30] P. M. Morse, *Thermal Physics*, 2nd edition (Benjamin/Cummings, Reading, MA, 1969).
- [31] F. Becattini, A. Giovannini, and S. Lupia, *Z. Phys. C* **72**, 43 (1996).
- [32] D. Stauffer and A. Aharony, *Introduction to Percolation Theory*, 2nd edition (Taylor and Francis, London, 1992).
- [33] U. Ornik, F. Pottag, R.M. Weiner, *Phys. Rev. Lett.* **63**, 2641 (1989).
- [34] B.R. Schlei, D. Strottman, and N. Xu, *Phys. Rev. Lett.* **80**, 3467 (1998).
- [35] L.D. Landau, E.M. Lifschitz, "Fluid mechanics" (Pergamon, New York, 1959).
- [36] J. Bolz, U. Ornik, R.M. Weiner, *Phys. Rev. C* **46**, 2047 (1992).
- [37] S. Wenig, Ph.D. thesis, GSI-Report 90-23 (October 1990).
- [38] J. Bolz, U. Ornik, M. Plümer, B.R. Schlei, R.M. Weiner, *Phys. Lett.* **B300**, 404 (1993).
- [39] J. Bolz, U. Ornik, M. Plümer, B.R. Schlei, R.M. Weiner, *Phys. Rev.* **D47**, 3860 (1993).
- [40] Th. Alber et al., *Phys. Rev. Lett.* **74**, 1303 (1995); Th. Alber et al., *Z. Phys.* **C66**, 77 (1995).
- [41] T. Alber for the Collaborations NA35 and NA49, *Nucl. Phys.* **A590**, 453c (1995); T. Alber et al., *Phys. Rev. Lett.* **75**, 3814 (1995).
- [42] N. Arbex, U. Ornik, M. Plümer, A. Timmermann and R.M. Weiner, *Phys. Lett.* **B345**, 307 (1995).
- [43] U. Ornik and R.M. Weiner, *Phys. Lett.* **B263**, 503 (1991).
- [44] Nu Xu for the NA44 Collaboration, *Nucl. Phys.* **A610**, 175c (1996).
- [45] I. G. Bearden et al. (NA44 Collaboration), *Phys. Lett.* **B388**, 431 (1996).
- [46] P.G. Jones and the NA49 Collaboration, *Nucl. Phys.* **A610**, 188c (1996).
- [47] K. Redlich, H. Satz, *Phys. Rev.* **D33**, 3747 (1986).
- [48] M. Gyulassy and S. K. Kaufmann, *Phys. Rev. Lett.* **40**, 298 (1978).
- [49] S. K. Kaufmann and M. Gyulassy, *J. Phys. A* **11**, 1715 (1978).
- [50] M. H. Quenoille, *Biometrics* **5**, 162 (1949).
- [51] S. Hegyi, *Phys. Lett. B* **309**, 443 (1993).

TABLE I. The probability P_N of N pions compared to a Poisson distribution with the same $\langle N \rangle$. Also given are the cycle class parameters x_k obtained from Eq. (14).

N	P_N	Poisson	k	x_k
0	.311	.293		
1	.346	.359	1	1.10812
2	.208	.221	2	.04812
3	.0903	.0904	3	.00588
4	.0320	.0278	4	.00107
5	.00998	.00682	5	.00024
6	.00287	.00139	6	.00006

TABLE II. The distribution of x_k in a Relativistic Hydrodynamic Model

k	x_k	k	x_k
1	260	6	.0067
2	9.957	7	.0016
3	1.047	8	.0004
4	.163	9	.0001
5	.031		

TABLE III. Values of x_k . Unless η is large, the x_k fall very rapidly and thus the $\langle N \rangle$ and $\langle N^2 \rangle - \langle N \rangle^2$ are governed by the first few k 's. For the coice $R^2/2 = 6$ and $1/8mT = 1/6$, the $\eta_c = 42.875$. However, the second $x_k = x_2$ is comparable to x_1 at $\eta = 432$, the x_3 to x_2 at $\eta = 140$, the x_4 to x_3 at $\eta = 90$, etc.

k	x_k	k	x_k
1	η	6	$\eta^6/2.43 \times 10^{10}$
2	$\eta^2/432$	7	$\eta^7/1.32 \times 10^{12}$
3	$\eta^3/6.07 \times 10^4$	8	$\eta^8/7.40 \times 10^{13}$
4	$\eta^4/5.47 \times 10^6$	9	$\eta^9/3.8 \times 10^{15}$
5	$\eta^5/3.91 \times 10^8$	10	$\eta^{10}/2.07 \times 10^{17}$

TABLE IV. Values of x_k in a thermal model using the same choice of R^2, T as in Table 2. The x_k is also written as η^k/b_k where $x_1 = \eta$ and b_k is a number that is given in the table. The results η^k/b_k are very similar to that of Table 3.

k	x_k	$x_k = \eta^k/b_k$
1	20	η
2	0.991	$\eta^2/404$
3	0.142	$\eta^3/6.21 \times 10^4$
4	0.309×10^{-1}	$\eta^4/5.17 \times 10^6$
5	00.835×10^{-2}	$\eta^5/3.83 \times 10^8$
6	00.257×10^{-2}	$\eta^6/2.57 \times 10^{10}$
7	000.869×10^{-3}	$\eta^7/1.47 \times 10^{12}$
8	000.312×10^{-3}	$\eta^8/8.20 \times 10^{13}$
9	000.118×10^{-3}	$\eta^9/4.34 \times 10^{15}$
10	0000.462×10^{-4}	$\eta^{10}/2.22 \times 10^{17}$

FIG. 1. Cycles and Clusters. In the mapping of a cycle class problem into a cluster problem and vice versa, the cycle length corresponds to the cluster size; the number of cycles of length k corresponds to the number of clusters with k nucleons. Also shown is the vector $\vec{n} = (n_1, n_2, \dots, n_A)$ as a block diagram. The number of vertical blocks is k , and the number of columns with k blocks is n_k . The total number of blocks is A .

FIG. 2. Various Parallels. Various parallels are shown which include the partitioning of an integer, a corresponding block picture, a cluster, a cycle class representation of each partition, and an equivalent harmonic oscillator excitation. Some places where these various columns appear are as follows: The partitions of an integer appears in counting the number of irreducible representation of the symmetric group. Block pictures and rotated versions of the ones shown appear in combinatorial analysis (Ferrer's block diagram) and in group theory (Young tableaux). Cluster problems appear in many areas of physics such as nuclear multifragmentation, percolation, randomly broken objects, and the fragmentation of atomic clusters. They also appear in group structure such as in the distribution of city sizes, etc. Cycle class problems appear in Bose-Einstein and Fermi-Dirac statistics, speckle patterns in phase space, Feynman's theory of the λ -transition in liquid He, in random permutations, etc. Excitations in the harmonic oscillator appear when evaluating the micro-canonical partition function of Bose atoms in a laser trap. Another application is to the Veneziano-Hagedorn mass spectrum, where each excitation is an elementary particle.

FIG. 3. Results for P_N for thermal pions, π^- , in 158 $A \cdot GeV$ Pb+Pb collisions. The solid line uses contributions $k \rightarrow 600$ (already $k = 10$ gives the fully converged result). The dotted lines only uses up to $k = 2$ terms. In the figure, we have (solid line) $\Sigma x_k = 271.2$, $\langle N \rangle = \Sigma k x_k = 283.9$, and $\langle N^2 \rangle - \langle N \rangle^2 = \Sigma k^2 x_k = 312.97$.

Figure 1:

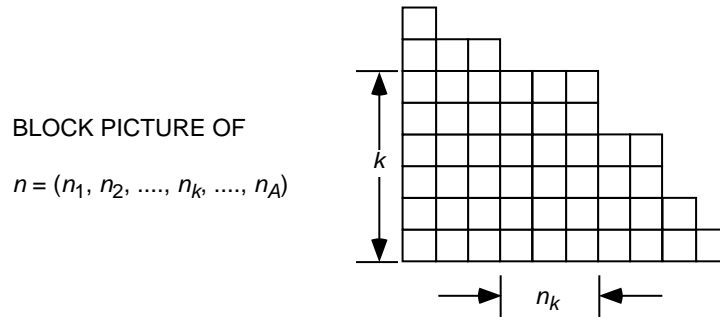
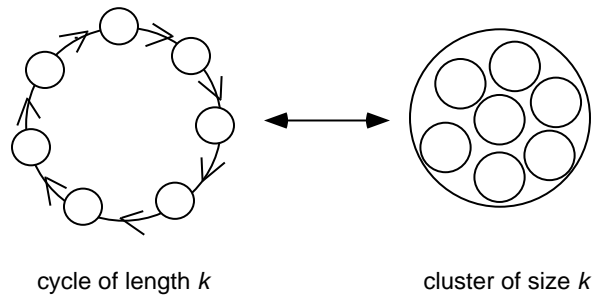


Figure 3:

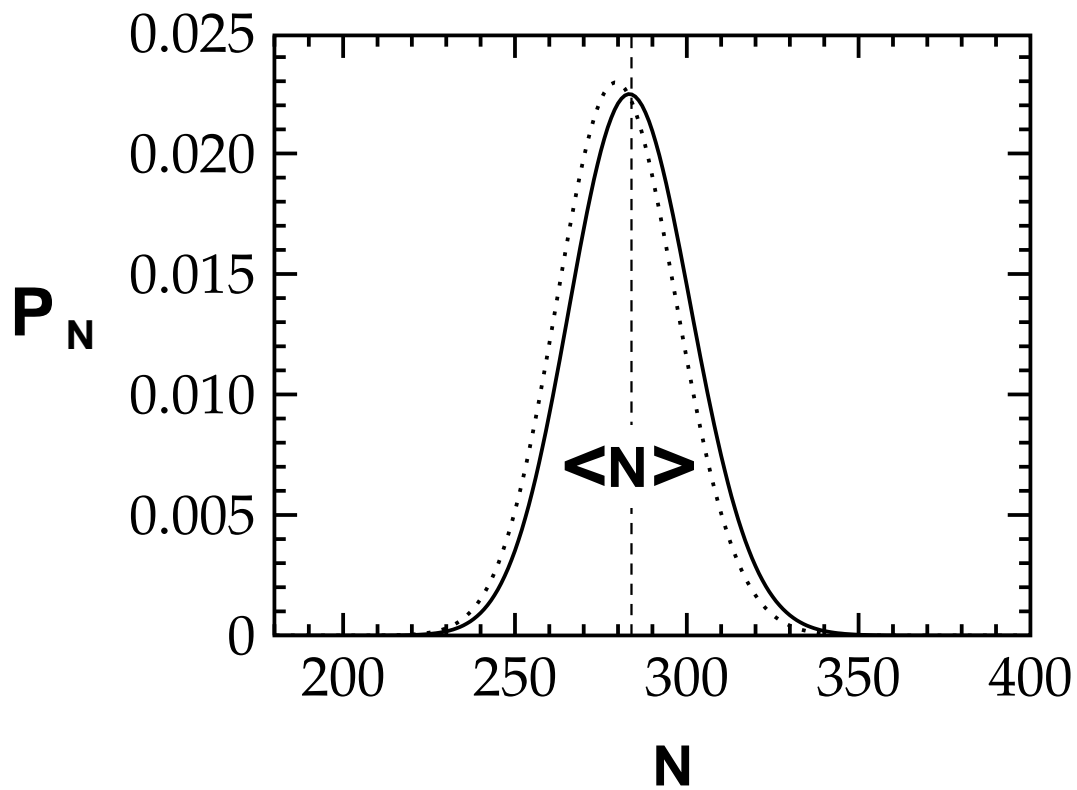
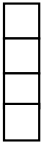
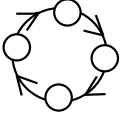
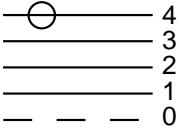
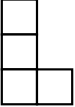
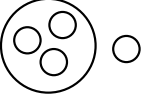
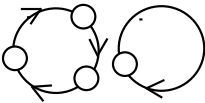
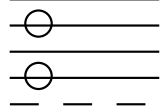
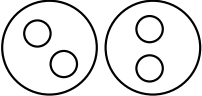
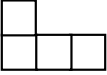
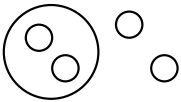
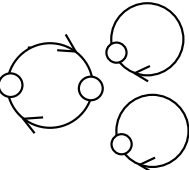
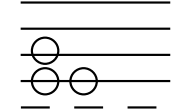


Figure 2:

Partitions of 4	Block Picture	Cluster Problem	Cycle Problem	Harmonic Oscillator
4				
3 + 1				
2 + 2				
2 + 1 + 1				
1 + 1 + 1 + 1		